

Sticking probability and mobility of a hydrogen atom on icy mantle of dust grains

Koichi Masuda¹, Junko Takahashi², and Tadashi Mukai¹

¹ The Graduate School of Science and Technology, Kobe University, Nada, Kobe 657, Japan

² Institute for Fundamental Chemistry, 34-4, Takano-Nishihiraki-cho, Sakyo-ku, Kyoto 606, Japan

Received 18 April 1997 / Accepted 12 September 1997

Abstract. The sticking and the diffusion processes of a hydrogen atom on the surface of icy mantle of dust grains have been investigated based on the classical molecular dynamics (MD) simulation. As the model for the icy mantle, a slab-shaped amorphous water ice with infinite area was generated by MD simulation under the periodic boundary condition. It was found that the densities and the oxygen-oxygen distance radial distribution function of our resulting amorphous water ice at 10 K and 70 K were in good agreement with those of the experimental high- and low- density amorphous water ice, respectively. By using the potential energy field for an incident H atom on our amorphous water ice, the dynamical behaviors of an impinging H atom on its surface were examined. From a statistic study for about 60 simulations in each cases, we have deduced that the sticking probability S_T of an incident H atom with a kinetic temperature T_h of 10 K, 100 K, and 350 K on 10 K ice were 1.0, 0.98, and 0.53, respectively. On 70 K ice, the values of S_T became 0.98, 0.86, and 0.52 for $T_h = 70$ K, 100 K, and 350 K, respectively. Our simulations have revealed that the impinging H atoms in the sticking cases diffused on the surface of ice by thermal hopping, and then they were trapped in one of potential wells on the icy surface. It was found, furthermore, that the mobility of the H atom before it became trapped nearly depends on the ice temperature. No ejection of the trapped H atom thermally occurred at least in our simulations.

Key words: diffusion – dust – molecular processes – ISM: molecules

1. Introduction

It is likely that a large number of molecules in space are formed on the surface of dust grains as has been suggested already by van de Hulst (1949). The fundamental processes of the surface chemistry on the dust grain are as follows: sticking of incident atoms or molecules, their diffusion over the surface, the surface reaction between them, and the retention of the products (Buch

1989, Williams 1993). In order to investigate the chemical processes on the grain surfaces, *e.g.*, H₂ formation, hydrogenation of molecules, and grain mantle formation, it is very important to find out the sticking probability and mobility of a hydrogen atom on it.

Hollenbach and Salpeter (1970) estimated the adsorption energy and mobilities of light gas atoms/molecules (He, H₂, H) on some surfaces (crystalline Ar and H₂O) by using simple quantum mechanical treatment, and represented an analytical expression for the sticking probability by classical treatment with the harmonic oscillator potential model. Leitch-Devlin and Williams (1985) calculated the sticking coefficients and the mobilities of adatoms (H, H₂, C, etc.) on the surface of crystalline solids (graphite, silicate, solid MgO as a metal oxide, etc.) with fully quantum mechanical treatment.

The dust grains generally have the icy mantles which accumulate on the solid particles inside the dark clouds. The astronomical observations tell us that the icy mantles are expected to be amorphous water ice rather than crystalline one (see, *e.g.*, Hagen et al. 1981). It is known that there are two forms for amorphous water ice, the high-density form and the low-density one. The high-density amorphous water ice was first discovered by Nartou et al. (1976) by their laboratory studies. Jenniskens and Blake (1994) and Jenniskens et al. (1995) identified it and modeled its structure.

The dynamical structures of amorphous water clusters were studied by Zhang and Buch (1990) and by Buch (1990) using classical molecular dynamics (MD) computational simulation. Buch and Zhang (1991) studied the sticking probability of H and D atoms on amorphous water clusters containing 115 water molecules by MD simulation. However, the cluster model made the structure of amorphous water ice too compact. The second peak position of the oxygen-oxygen distance radial distribution function for their amorphous water ice was shifted to a shorter distance than the experimental one (Zhang and Buch, 1990). Moreover, their cluster which contained only 115 molecules was considered to be rather small to represent the mantle surface of dust grains.

Recently, as the more realistic model for the icy mantle of dust grains, Masuda and Takahashi (1997) generated a slab-shaped amorphous water ice with infinite area by MD simulation under the periodic boundary condition, where the slab in a unit cell had about $40 \text{ \AA} \times 40 \text{ \AA} \times 20 \text{ \AA}$ volume and contained 1000 water molecules in it. And, a preliminary study was done for the behavior of a hydrogen atom thrown onto the slab surface.

Classical MD simulation is the well established technique for studying molecular processes in the field of physical chemistry. This technique is based on the numerical solutions of Newton equations of motion for a many-body system. Despite the limit of the classical treatment of the motions, it has provided us with many realistic information about the molecular processes, *e.g.*, water dynamics, when they are dominated by the thermal dynamics (see, *e.g.*, Hansen and McDonald 1986). Our model, where the hydrogen atom is physisorbed on the surface of the icy mantle and has excess thermal energy during the processes of interest, could be also well treated by this technique (Masuda and Takahashi 1997). The quantum treatment is necessary only for the process after the H atom loses the excess thermal energy and becomes trapped on the surface of dust grains (Takahashi et al., 1997).

In the present work, we have investigated the sticking probability and the mobility of an incident H atom on the icy mantle of dust grains by classical MD simulation. The slab-shaped amorphous water ice with the infinite area was generated by MD simulation using the periodic boundary condition, as the model surface of the icy mantle of dust grains. The potential energy field for an incident H atom on the amorphous water ice was examined. Then, MD simulation about the H atom thrown onto the surface of amorphous water ice was performed to study its dynamical behavior on it. We studied the temperature dependences of the structure of amorphous water ice and of the sticking probability and the mobility of the impinging H atom. The computational procedure is argued in Sect. 2, the results and discussion are in Sect. 3, and the conclusions are summarized in Sect. 4.

2. Computational procedure

For the first stage of our simulation, the amorphous water ice slab was generated by MD simulation under the three-dimensional periodic boundary condition. As the initial conditions, 1000 water molecules were placed randomly in the range of $-15 \text{ \AA} < z < +15 \text{ \AA}$ in the unit cell of about $40 \text{ \AA} \times 40 \text{ \AA} \times 40 \text{ \AA}$ volume, where $z = 0$ was taken at the plane including the center of the cell. The time step of the MD simulation was taken to be 1 fs (femtosecond). With the passage of time, the water molecules grew concentrated into the region of $-10 \text{ \AA} < z < +10 \text{ \AA}$ by the attractive forces between each other. After 10 ps (picoseconds) (= 10,000 fs) run, an amorphous water ice slab with the thickness of 20 \AA was produced and its structure was considered to be in equilibrium. Thus, the resulting slab (see Fig. 1) was found to have the two-dimensional periodic boundary condition in x and y directions.

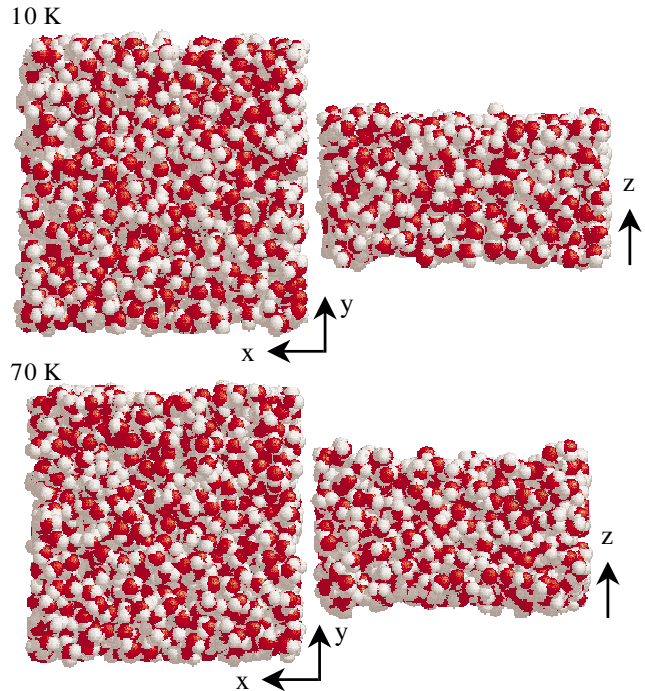


Fig. 1. The amorphous water ice slabs generated by our MD simulations at 10 K and 70 K. Left pictures indicate upper views and right ones side views. The white and black balls mean oxygen and hydrogen atoms in water molecules, respectively. The volume is about $40 \text{ \AA} \times 40 \text{ \AA} \times 20 \text{ \AA}$. In this coordinate system, the origin is at the center of the slabs and the periodic boundary condition was employed in the x and y directions.

The water molecules were treated as rigid, and Leap-Frog procedure was used in the algorithm of integration. The potential model used for pairs of water molecules was TIPS2 (Transferable Intermolecular Potential of the second version) by Jorgensen (1982):

$$V_{H_2O-H_2O} = \frac{A}{r_{OO}^{12}} - \frac{B}{r_{OO}^6} + \sum_i \sum_j \frac{q_i q_j e^2}{r_{ij}} \quad (1)$$

This equation consists of the Lennard-Jones part (the first and the second terms) and the Coulomb part (the third term). In the Lennard-Jones part, r_{OO} indicates the distance between the oxygen atoms in a pair of water molecules. Parameters A and B are $695,000 \text{ kcal \AA}^{12}/\text{mol}$ and $600 \text{ kcal \AA}^6/\text{mol}$, respectively. In the Coulomb part, i and j indicate the positions of three charges which are defined as two positive charges ($q_H = 0.535e$; e denotes an elementary charge) located at the hydrogen atoms and one negative charge ($q_O = -2q_H$) at a distance of 0.15 \AA from the oxygen atom on the bisector of the H–O–H angle.

The amorphous water ice slabs were generated for two temperatures, 10 K and 70 K. The temperatures of the slabs were always kept nearly constant by rescaling the velocities of water molecules during this simulation.

For the second stage of our simulation, we performed MD simulation for the system consisting of the amorphous water

Table 1. Parameters for the pair potential between a hydrogen atom and a water molecule (after Buch and Zhang 1991)

l, m	$\varepsilon_{l,m}$ [kcal/mol]	$\sigma_{l,m}$ [Å]
0, 0	0.44106	3.00
1, 0	-0.03884	3.30
2, 0	0.03515	2.98
2, 2	0.14549	2.92

ice slab and an H atom thrown onto it, where the equations of motion for 1000 water molecules and an H atom were solved under the periodic boundary condition. The procedure of the simulation was essentially the same as that of the first stage.

For the additional potential between an H atom and an H₂O molecule, Zhang-Sabelli-Buch potential model (Zhang et al., 1991) was employed. This potential function consists of the Lennard-Jones part and the spherical harmonic function $Y_{l,m}$ in the following way.

$$V_{H-H_2O} = \sum_{l,m} 4\varepsilon_{l,m} \left[\left(\frac{\sigma_{l,m}}{r} \right)^{12} - \left(\frac{\sigma_{l,m}}{r} \right)^6 \right] Y_{l,m}(\theta, \phi) \quad (2)$$

In this equation, r , θ , and ϕ indicate the position of the incident H atom. The coordinate system is a spherical one whose origin is located on oxygen atom. Two H atoms in a water molecule are placed on $R = 0.9572$ Å, $\theta = 127.74^\circ$, and $\phi = \pm 90^\circ$. The detail of parameters ($\varepsilon_{l,m}$ and $\sigma_{l,m}$) are shown in Table 1.

The initial kinetic temperatures of the impinging H atoms T_h were chosen to be 10 K, 100 K and 350 K on the 10 K amorphous water ice and 70 K, 100 K and 350 K on the 70 K ice. For the initial positions of the impinging H atom, the value of z was kept ± 20 Å and the values of x and y were randomly selected, where the surface of the amorphous water ice slab was located at about $z = \pm 10$ Å. The temperature rescaling of the ice was continued during this simulation. The time step was 1 fs, and the duration of the trajectories followed was 5000 fs.

3. Results and discussion

3.1. Amorphous water ice

It is known that the amorphous water ice has two different forms (Jenniskens and Blake 1994). Below 38 K, the amorphous water ice is in high density form (about 1.1 g/cm³). As it is warmed up from 38 K to 68 K, its density decreases gradually. Over 68 K, it is in low density form (about 0.94 g/cm³).

The amorphous water ice slabs produced by our MD simulations are shown in Fig. 1. It was found that the slab at 70 K seemed to be looser than that at 10 K. Actually, the density at 10 K was about 1.07 g/cm³ while that at 70 K was about 0.93 g/cm³.

In order to check that these slabs could reproduce real amorphous water ice, we compared the oxygen-oxygen distance radial distribution functions of our slabs with those obtained experimentally by Jenniskens et al. (1995), as shown in Fig. 2. The first peaks at both 10 K and 70 K were sharp and their positions

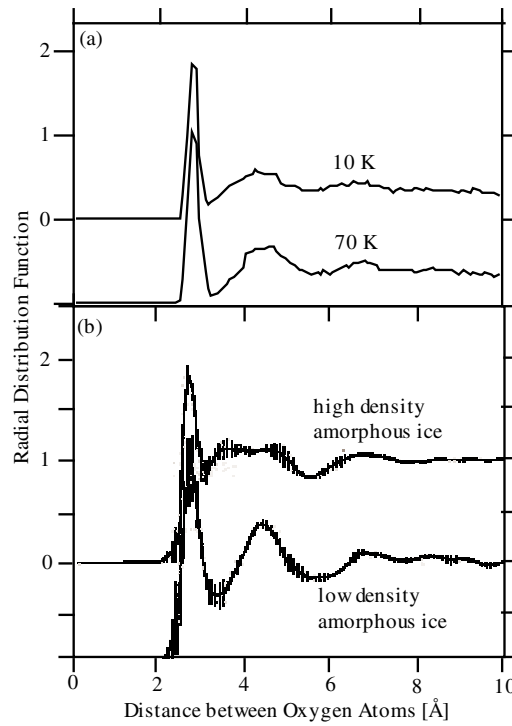


Fig. 2a and b. Oxygen-oxygen distance radial distribution function; **a** results for our slabs; **b** experimental electron diffraction results obtained by Jenniskens et al. (1995).

were at 2.8 Å. It was in good agreement with the first peaks of the experiments at both 14 K (2.8 Å) and 77 K (2.8 Å). It was also consistent with the first nearest neighbor distance of crystalline water ice, 2.76 Å. The second peak of our 10 K ice was broad and looked like an assembly of several peaks in the range of about 3.6 Å to 4.8 Å. Experimentally, the second peak at 14 K was split into two broad peaks at 3.7 Å and 4.7 Å. The character of the former spectra is considered to reproduce that of the latter. The second peak of our 70 K ice was narrow and its position was at 4.4 Å, which was in good agreement with that of the experiment at 77 K (4.4 Å).

Judging from the agreements of the densities and the radial distribution functions between our ice and experimental one, we conclude that the amorphous water ice slabs produced by our MD simulations are the good analogues for the amorphous water ice mantle of dust grains.

3.2. Potential energy field of H atom on ice

Before the dynamical studies on an incident hydrogen atom on amorphous water ice, we investigated the potential energy field for the present system. The results for an H atom on 70 K ice are shown in Fig. 3. Fig. 3a-e are the contour maps of the potential energy surface when an H atom exists on the planes of $z = 9 \sim 13$ Å, where $z = 0$ indicates the plane including the center of the slab. The positive potential energy region (the slashed region) indicates the area spatially occupied by water molecules as well as where the impinging H atom is un-stabilized by the surface

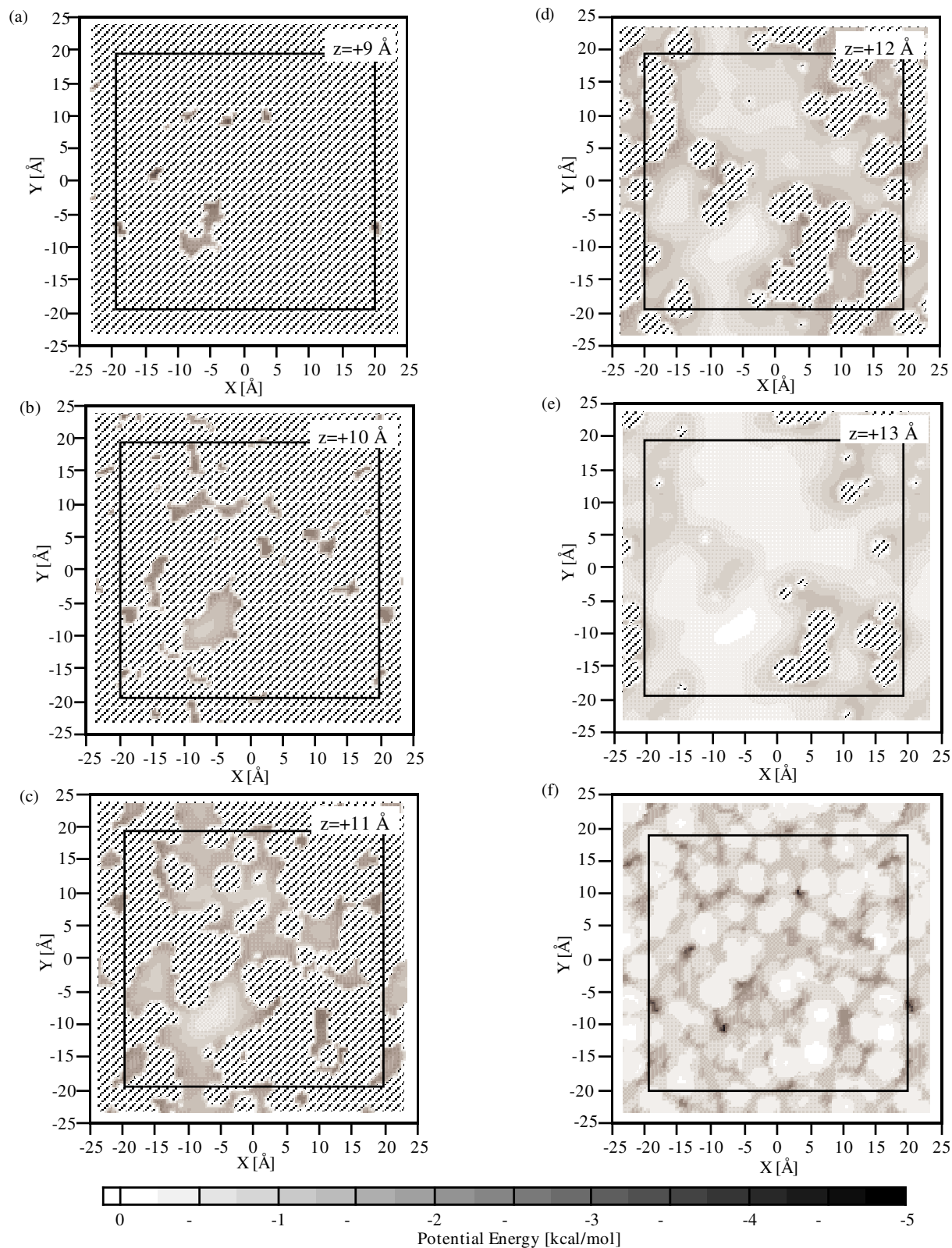


Fig. 3a–f. Potential energy field of an incident hydrogen atom near the surface of 70 K amorphous water ice. **a–e** are the contour maps of the potential energy surface when an H atom exists on the planes of $z = 9\sim 13 \text{ \AA}$, where $z = 0$ indicates the plane including the center of the slab. The potential is positive in the slashed region and negative in other regions. The darker the gradient is, the more negative the potential energy becomes. **f** is an image of the potential energy field which was made of the superposition of **a–e**. The rectangle in each figure indicates the size of unit cell.

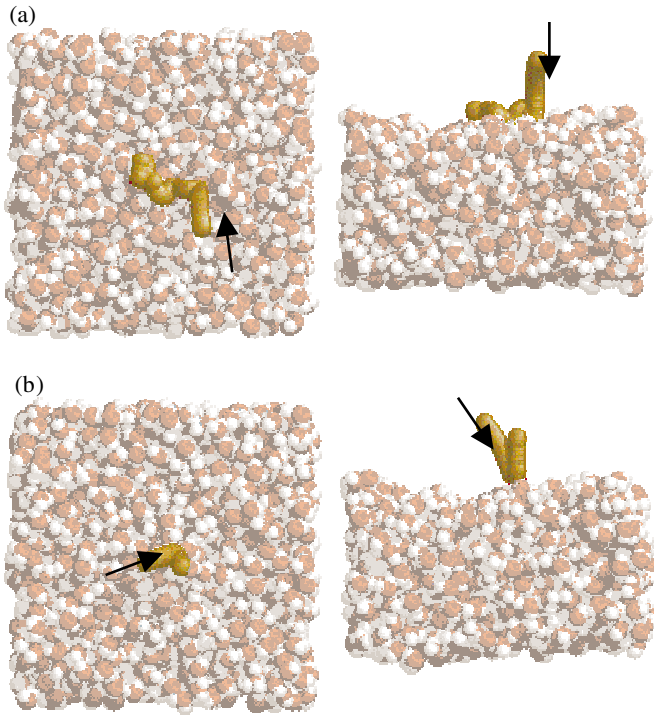


Fig. 4a and b. Two samples of MD trajectories of incident hydrogen atoms on the amorphous water ice slab; **a** the sticking case for 10 K H atom on 10 K ice; **b** the scattered case for 100 K H atom on 70 K ice. A dark silver tube means the trajectory of an incident H atom. Arrows indicate the starting position and the direction of an incident H atom.

of ice. In the negative potential energy region (the gradient region), the impinging H atom is stabilized by water molecules of ice. The stabilization energy between an H atom and a water molecule is about 0.3 kcal/mol (Zhang et al. 1991).

At $z \leq 11$ Å (Fig. 3a-c), since there were more water molecules at those heights, the area of the positive potential energy region became larger and larger. And the negative potential energy region became deeper because many water molecules could be around the impinging H atom and stabilize it much greatly. At $z \geq 12$ Å (Fig. 3d-e), the area of the positive potential energy region was small and the negative potential energy region was shallow, because an impinging H atom was for the most part above the surface of ice. This means that the deeper potential energy regions are at spatially deeper region. The minimum potential energy for an H atom on 70 K ice was about -5 kcal/mol, which was found on the $z = 9$ Å plane. Fig. 3f is an image of the potential energy field which was made of the superposition of figures (a)–(e). From this figure, we could gain the global information about the potential energy field near the surface of the amorphous water ice and find the positions of potential wells.

The potential energy field of an H atom on 10 K amorphous water ice was similar to that on 70 K ice. However, the irregularity of the surface of 10 K ice was less than that of 70 K because the density of 10 K ice was higher and water molecules were more packed into the slab (*cf.* the difference of the second peak in Fig. 2).

3.3. Sticking probability

The results of our MD simulations for the amorphous water ice slab and an H atom thrown onto the surface of it were classified into the two cases. One was the sticking case where an incident H atom resided on the surface of the amorphous water ice after 5000 fs (Fig. 4a). Another was the scattered case (Fig. 4b). We considered that an incident H atom was scattered when it went back to the initial height ($z = 20$ Å) within 5000 fs. As for the sticking case, it was found to take about 3000 fs until the temperature of adsorbed H atoms became in equilibrium with the slab temperature. Therefore, we considered that 5000 fs of the simulation period was adequate for these simulations. From a statistic study for about 60 simulations in each cases, we have deduced the sticking probability S_T of an incident H atom with a kinetic temperature T_h . In Table 2, summary of the results and the estimated sticking probabilities are shown. We denote by T_{ice} and T_h temperature of the amorphous water ice and the incident H atom, respectively. N_{total} and $N_{sticking}$ represent the total number of calculated trajectories and the number of trajectories which resulted in sticking at given T_{ice} and T_h , respectively. Here, we also estimated statistical uncertainties for the sticking probabilities, which were calculated based on the method that was adopted in the work by Buch and Zhang (1991).

In the scattered cases, most of H atoms were rebounded from the surface of ice immediately after the encounter. However, in some of the cases, the incident H atom was ejected from the ice after bounding three or four times on the surface. This results means that the scattered H atoms were ejected before the energy transfer from the H atoms to the amorphous water ice occurred adequately, as argued in the next section.

Buch and Zhang (1991) studied the sticking process of H and D atoms on the cluster-type amorphous water ice, and they found that the sticking probability S_T at a gas temperature T was approximately given by

$$S_T = (k_B T / E_0 + 1)^{-2}, \quad (3)$$

where $E_0 = 102$ K for H atoms and k_B denotes Boltzmann constant. According to this expression, the sticking probabilities on the 8–10 K ice were 0.83, 0.25, and 0.05 for 10 K, 100 K, and 350 K incident H atoms, respectively.

The analytical expression by Hollenbach and Salpeter (1970), using simple harmonic oscillator model, is approximately given by

$$S_T = (\gamma^2 + 0.8\gamma^3) / (1 + 2.4\gamma + \gamma^2 + 0.8\gamma^3), \quad (4)$$

$$\gamma \equiv \Omega(D\Delta E_S)^{1/2} / k_B T,$$

where Ω is a parameter indicating the character of the scattering process ($\Omega^2 \simeq 1$ for Lambert's law and $\Omega^2 \simeq 2$ for isotropic scattering above surface), D is an attractive adsorption potential well depth, and ΔE_S denotes the amount of energy transferred from the impinging atom to the surface during one hopping process. They employed $D = 300$ K and $\Delta E_S = 17$ K for the system of an H atom and the crystal water ice.

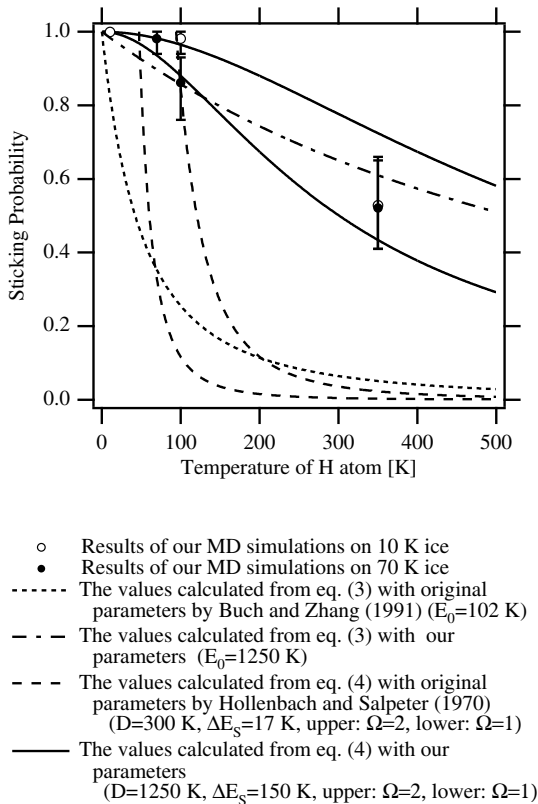


Fig. 5. Sticking probability as a function of temperature of the incident hydrogen atom on the water ice.

In order to obtain the sticking probability as a function of temperature, we estimated suitable parameters in Eqs. (3) and (4) for our system consisting of an H atom and the slab-shaped amorphous water ice; $E_0 = D \simeq 1250$ K and $\Delta E_S \simeq 150$ K. Our results are shown in Fig. 5 together with the results by Buch and Zhang (1991) and by Hollenbach and Salpeter (1970).

We found that the values of sticking probability calculated from Eqs. (3) and (4) with using our parameters were almost well fitted with our MD simulation results. However, the values calculated from Eq. (3) with using their original parameters were rather smaller than ours at any temperatures. It is considered that the large irregularity in shape of their amorphous water ice cluster made it more difficult for incident H atoms to stick on it, while our slab-shaped amorphous water ice with infinite area should be more sticky. The values of sticking probability calculated from Eq. (4) with using their original parameters were also rather smaller than ours at higher temperatures. The factor affecting the values is the difference in the potential between our amorphous water ice and their crystal water ice. Nevertheless, Eq. (4) was adequately applicable to our model by only changing the parameters of the equation.

3.4. Mobility

In the sticking cases, the impinging H atoms diffused on the surface of the amorphous water ice slab and became trapped

Table 2. Sticking probability of incident hydrogen atom on ice. The maximum and minimum values for sticking probabilities at the 95% confidence level are also shown.

T_{ice}	T_h	N_{total}	$N_{sticking}$	S_T (Min. – Max.)
10 K	10 K	59	59	1.00
10 K	100 K	62	61	0.98 (0.94 – 1.00)
10 K	350 K	57	30	0.53 (0.41 – 0.66)
70 K	70 K	62	61	0.98 (0.94 – 1.00)
70 K	100 K	64	55	0.86 (0.76 – 0.93)
70 K	350 K	65	34	0.52 (0.41 – 0.65)

in one of stable sites on the surface of it. The trapped sites correspond to the potential wells which were argued in Sect. 3.2.

Two samples for time dependence of the position height, the kinetic energy, the potential energy, and the total energy of the impinging H atom are shown in Fig. 6a-d are for 10 K ice and Fig. 6e-h are for 70 K ice. For both samples, the initial kinetic energy of the impinging H atom T_h was 100 K. The height (position in the z -direction) of the impinging H atom was measured from the plane including the center of the amorphous water ice slab. The surface of amorphous water ice was roughly estimated to be around 10 \AA height. The potential energy means the interaction energy between the impinging H atom and the amorphous water ice.

The vertical thick lines in Fig. 6 indicate the time when the impinging H atom came into contact with the surface of ice at first. In the diffusion process at the first stage, it was seen that the impinging H atom was hopping on the surface of ice. The alternative transfer between potential energy and kinetic energy of H atom was also seen. The average total energy of impinging H atom was found to be gradually decreased, because a part of energy would be absorbed by amorphous water ice during H atom's hopping process. It was seen that the fluctuation of energies was more intense for 70 K ice than for 10 K ice.

The vertical dotted lines in Fig. 6 indicate the time when the H atom became trapped in one of potential energy wells on the surface of ice. The potential energy at the trapped sites was about -4 kcal/mol for both samples. After the impinging H atom was trapped, the average total energy of the H atom in this stage was found to be sufficiently smaller than that of initial energy of the incident H atom. It was seen that the fluctuation of kinetic energy was also small and would never go up to the potential energy barrier of the well. Thus, it is found to be very difficult that the trapped H atoms move to another attractive site on the surface of ice.

In order to evaluate the mobility of adsorbed H atoms before they lose the excess thermal energy and become trapped, we measured the migration lengths and times along the MD trajectories of the impinging H atom, starting from the first contacting position s with the surface and ending at the trapped positions. The results are listed in Table 3 based on the number of simulations given in Table 2. It was found that the averages of migration lengths and times nearly depend on the slab temperatures. The H atoms on 70 K ice were mobiler than those

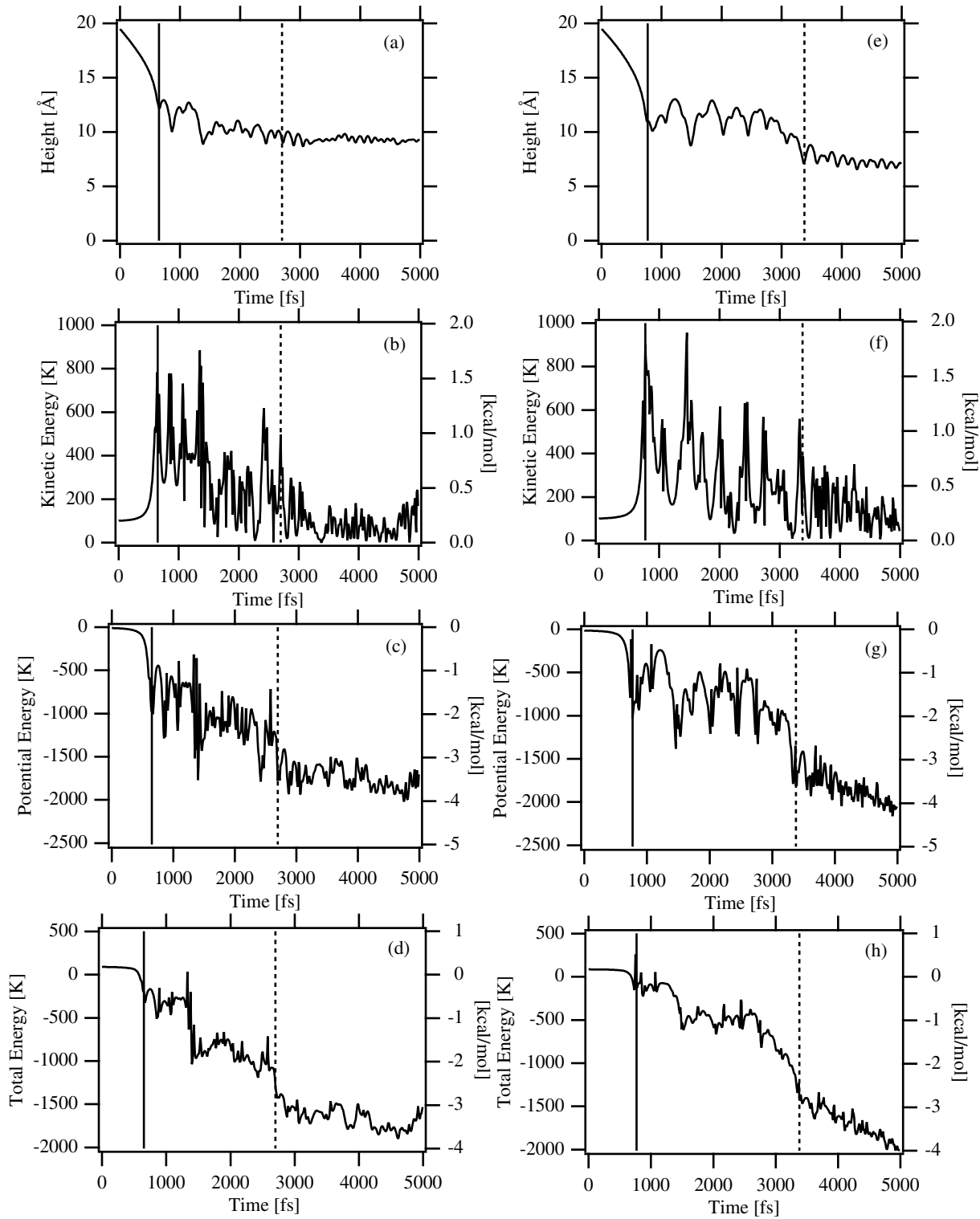


Fig. 6a–h. Time dependence of the height, the kinetic energy, the potential energy, and the total energy of the impinging hydrogen atom for two samples; **a, b, c,** and **d** are for 10 K ice and **e, f, g,** and **h** are for 70 K ice. For both samples, the initial kinetic energy of the impinging H atom T_h was 100 K. Vertical thick lines indicate the time when the impinging H atom came into contact with the surface of ice at first (650 fs for 10 K ice and 770 fs for 70 K ice). Vertical dotted lines indicate the time when the H atom was trapped on the surface of ice (2750 fs for 10 K ice and 3380 fs for 70 K ice). The migration lengths for these samples, which are defined as the length of MD trajectory from the first contacting position (thick line) to the trapped position (dashed line), are 96.90 Å and 157.19 Å, respectively.

Table 3. Mobility of incident hydrogen atom on ice. The migration length and time are represented by (an average value) \pm (a standard deviation).

T_{ice}	T_h	Migration length [\AA]	Migration time [fs]
10 K	10 K	60.40 \pm 39.50	1682.81 \pm 750.50
10 K	100 K	61.36 \pm 50.06	1796.41 \pm 564.44
10 K	350 K	86.15 \pm 72.12	2045.00 \pm 498.99
70 K	70 K	140.12 \pm 130.72	2688.61 \pm 1241.93
70 K	100 K	143.72 \pm 181.15	2556.18 \pm 1300.83
70 K	350 K	154.26 \pm 102.61	3562.22 \pm 1435.86

on 10 K ice. There is relatively weak dependence on the initial temperatures of the incident H atoms.

In order to evaluate the mobility of adsorbed H atoms after they are trapped, we performed the MD simulations until 50 ps. However, we found that none of H atoms which have been once trapped on the surface were restarted to diffuse. For the diffusion process via thermal hopping mechanism, the time scale for a particle moving to a neighboring site τ_h is estimated by

$$\tau_h = \nu^{-1} \exp(T_b/T_{ice}), \quad (5)$$

where ν is the frequency of classical oscillation parallel to the surface, $k_B T_b$ is the height of the barrier to motion, and T_{ice} is the temperature of amorphous water ice (Williams 1993). From the simulations shown in Fig. 6, we found $\nu \approx 0.01 \text{ fs}^{-1}$ and $T_b \approx 1250 \text{ K}$. By using these parameters, we could obtain $\tau_h \approx 10^{34}$ years for 10 K ice and $\tau_h \approx 10^{-5}$ seconds for 70 K ice. Therefore, the mobility of adsorbed H atoms after they are trapped on 10K ice via thermal hopping mechanism is estimated at nearly zero, while it is considered that adsorbed H atoms after they are trapped on 70K ice could rediffuse thermally.

Actually, the mobility after H atoms are trapped might be underestimated by classical theory, because the H atom under the very low temperature condition could diffuse more effectively via quantum tunneling mechanism. In future work, we will calculate the quantum mechanical diffusion constant for an H atom over the surface of amorphous water ice, where the tunneling effects are accurately included (Takahashi et al., 1997).

4. Conclusions

In this paper, we investigated the sticking and the diffusion processes of a hydrogen atom on the surface of the icy mantle of dust grains by using classical MD simulations.

At first, we produced the slab-shaped amorphous water ice with infinite area by MD simulation using the periodic boundary condition. The resulting amorphous water ice slabs at 10 K and 70 K were found to be in good agreement with the experimental data about the densities and the radial distribution functions for high- and low- density amorphous water ice, respectively. We regarded our amorphous water ice slab as the realistic model for the icy mantle of dust grains.

The potential energy field for an incident hydrogen atom on the amorphous water ice was examined. It was found that

several potential wells located randomly on the surface of the ice. The maximum depth of them was about -5 kcal/mol .

The sticking probabilities of the incident H atoms with kinetic temperatures T_h of 10 K and 100 K on our 10 K amorphous water ice slab were unity and 0.98, respectively, while those with $T_h = 70 \text{ K}$ and 100 K on 70 K ice were 0.98 and 0.86, respectively. The sticking probabilities of the incident H atoms with $T_h = 350 \text{ K}$ on both 10 K and 70 K amorphous ice were about 0.5. There was the tendency for the sticking probability to decrease as the temperature both of amorphous water ice and of incident H atom increases. Our MD simulation results were almost well fitted with expressions for the sticking probability as a function of temperature given by Buch and Zhang (1991) and by Hollenbach and Salpeter (1970), using modified parameters for our amorphous water ice model.

In the sticking cases, the impinging H atoms diffused on the surface of amorphous water ice initially via thermal hopping mechanism and then became trapped in one of potential wells on the surface. As for the mobility of H atoms before they were trapped, it was found that the migration lengths and times along their trajectories, measured from the first contacting positions with the surface to the trapped positions, mainly depended on the temperature of amorphous water ice. After the H atoms were trapped, it was found that the H atoms diffused no further and were never ejected from the surface thermally on 10 K ice while they could rediffuse thermally on 70 K ice.

Acknowledgements. We thank Dr. Atto Laaksonen of IBM Corp. for his code in the CCP5 program library in the computer center of Kyoto University, which we utilized as a part of our code. We are grateful to Dr. Masataka Nagaoka of Institute for Fundamental Chemistry, Dr. Ryosuke Nakamura of Kobe University, and Prof. Akira Kouchi, Dr. Naoki Watanabe, and Prof. Tetsuo Yamamoto of Hokkaido University for their helpful discussions. We are also grateful to Prof. Kenichi Fukui of Institute for Fundamental Chemistry for his encouragement. This work was partially supported by Research Fellowships of the Japan Society for the Promotion of Science for Young Scientists and by Hayashi Memorial Foundation for Female Natural Scientists. The computational simulations were carried out on NEC SX-4/1C supercomputer at Institute for Fundamental Chemistry and on NEC SX-3/34R at the Computer Center of Institute for Molecular Science.

References

- Buch, V., 1989, Evolution of Interstellar Dust and Related Topics, eds. A. Bonetti et al., 321.
- Buch, V., 1990, J. Chem. Phys., 93, 2631.
- Buch, V., and Zhang, Q., 1991, ApJ, 379, 647.
- Hagen, W., Tielens, A.G.G.M., Greenberg, J.M., 1981, Chem. Phys., 56, 367.
- Hansen, J.P., and McDonald, I.R., 1986, Theory of Simple Liquids (2nd edition) (New York: Academic Press)
- Hollenbach, D., and Salpeter, E.E., 1970, J. Chem. Phys., 53, 79.
- Jenniskens, P. and Blake, D.F., 1994, Sci, 265, 709.
- Jenniskens, P., Blake, D.F., Wilson, M.A., and Pohorille, A., 1995, ApJ, 455, 389.
- Jorgensen, W.L., 1982, J. Chem. Phys., 77, 4156.
- Leitch-Devlin, M.A., and Williams, D.A., 1985, MNRAS, 213, 295.
- Masuda, K., and Takahashi, J., 1997, Adv. Space Res., 19, 1019.

- Narten, A.H., Venkatesh, C.G., and Rice, S.A., 1976, *J. Chem. Phys.*, 64, 1106.
- Takahashi, J., Nagaoka, M., and Masuda, K. 1997, *Int. J. Quantum Chem.*, submitted.
- van de Hulst, H.C., 1949, *Rech. Astron. obs. Utrecht*, XI, part II.
- Williams, D.A., 1993, in *Dust and Chemistry in Astronomy*, ed. T.J.Millar and D.A.Williams, Institute of Physics Publishing, Philadelphia., pp.143-170.
- Zhang, Q., and Buch, V., 1990, *J. Chem. Phys.*, 92, 5004.
- Zhang, Q., Sabelli, N., and Buch, V., 1991, *J. Chem. Phys.*, 95, 1080.